JPhys Materials

TOPICAL REVIEW • OPEN ACCESS

Experimental advances in charge and spin transport in chemical vapor deposited graphene

IOP Publishing J. Phys. Mater. 4 (2021) 042007 https://doi.org/10.1088/2515-7639/ac1247

Journal of Physics: Materials

OPEN ACCESS

RECEIVED
31 December 2020

REVISED
3 June 2021

ACCEPTED FOR PUBLICATION
7 July 2021

PUBLISHED
19 August 2021

TOPICAL REVIEW

Experimental advances in charge and spin transport in chemical vapor deposited graphene

H Mishra[1], J Panda[1], M Ramu[2], T Sarkar[2], J-F Dayen[3,4], Daria Belotcerkovtceva[1] and M Venkata Kamalakar[1,*]

[1] Department of Physics and Astronomy, Uppsala University, Box 516, SE-751 20 Uppsala, Sweden
[2] Department of Materials Science and Engineering, Uppsala University, Box 35, SE-751 03 Uppsala, Sweden
[3] Institut de Physique et Chimie des Matériaux de Strasbourg, Université de Strasbourg, CNRS UMR 7504, 23 rue du Loess, BP 43, Cedex 2, F-67034 Strasbourg, France
[4] Institut Universitaire de France, 1 rue Descartes, 75231 Paris cedex 05, France
[*] Author to whom any correspondence should be addressed.

E-mail: venkata.mutta@physics.uu.se

Keywords: CVD graphene, ballistic transport, spin transport, flexible 2D spintronics, graphene spintronics

Abstract

Despite structural and processing-induced imperfections, wafer-scale chemical vapor deposited (CVD) graphene today is commercially available and has emerged as a versatile form that can be readily transferred to desired substrates for various nanoelectronic and spintronic applications. In particular, over the past decade, significant advancements in CVD graphene synthesis methods and experiments realizing high-quality charge and spin transport have been achieved. These include growth of large-grain graphene, new processing methods, high-quality electrical transport with high-carrier mobility, micron-scale ballistic transport, observations of quantum and fractional quantum Hall effect, as well as the spintronic performance of extremely long spin communication over tens of micrometers at room temperature with robust spin diffusion lengths and spin lifetimes. In this short review, we discuss the progress in recent years in the synthesis of high-quality, large-scale CVD graphene and improvement of the electrical and spin transport performance, particularly towards achieving ballistic and long-distance spin transport that show exceptional promise for next-generation graphene electronic and spintronic applications.

1. Introduction

Since its experimental isolation [1], graphene has emerged as an extraordinary modern material for its superlative electrical and thermal conductivity, mechanical strength, and unique optical properties [2]. Of particular importance for device applications are its high carrier mobility, charge, and spin transport attributes. These properties originate from graphene's unique electronic structure first discussed half a century ago by Wallace [3]. The uniqueness of graphene begins with its structure, a single atomic layer of sp^2 hybridized carbon atoms arranged in a two-dimensional honeycomb lattice that leads to a gapless electronic band structure with conduction and valence bands touching at the Dirac points. In addition, the linear symmetric electronic dispersion at lower energies makes charge carriers in graphene behave like relativistic massless Dirac fermions with Fermi velocity $v_F = 10^6$ m s^{-1} (1/300 times the speed of light) and results in ambipolar functionality [2]. Thus, the charge carriers possess very high mobility, and external electric fields can tune their concentration and polarity. Furthermore, the fact that its hexagonal lattice can be described by two interpenetrating triangular sublattices (A and B) leads to valley degeneracy $g_v = 2$ and an additional degree of freedom called pseudospin and chirality of the massless Dirac fermions. As a consequence of these unique attributes, graphene shows fascinating quantum transport phenomena of anomalous integer quantum Hall effect at relatively low fields [4], fractional quantum Hall effect [5, 6], Klein tunneling with unit transmission probability [7], the existence of minimal conductivity [8], and micrometer ballistic transport lengths [9, 10]. In addition to these properties, from the perspective of spintronics, graphene has two crucial traits: a weak spin–orbit coupling and negligible hyperfine interaction [2], which make graphene

an ideal medium for transport of spin-polarized currents, with theoretically predicted spin diffusion length ~100 μm at room temperature [11]. This has led to the field of graphene spintronics, starting from initial reports of micrometer-scale spin transport and precession [12] to tens of microns of spin current communication, with several nanoseconds (ns) spin lifetime, including flexible graphene spin devices [13].

The scientific community has explored the synthesis of graphene using different top-down and bottom-up methods like mechanical exfoliation, chemical exfoliation, epitaxial growth, molecular beam epitaxy, and chemical vapor deposition (CVD) [14–16]. Most experimental investigations employ graphene crystals obtained by mechanical exfoliation from highly oriented pyrolytic graphite and Kish graphite by the so-called 'scotch tape' method. In addition to this widely utilized scotch tape method, two other essential kinds of chemically grown graphene are epitaxial graphene produced over SiC substrates and CVD graphene grown on metal foils. In contrast to mechanical exfoliation that does not allow the control of sample quality and scale, the latter techniques provide scope for uniformity and scalability. The epitaxial growth of graphene was achieved by thermal decomposition of the (0001) face of a 6 H—SiC wafer in an ultrahigh vacuum [17], after which it was structured by lithography and characterized by various methods such as scanning tunneling microscopy, low energy electron diffraction, Raman spectroscopy, and transport measurements [18]. It was shown that the graphene grown on the silicon face (0001) has lower mobility of charge carriers than that grown on the silicon face $(000\bar{1})$ [19], which has been attributed to oxidizing gases causing defects. Compared to other graphene forms, the epitaxial samples have shown stronger interaction with the SiC substrate [20], which imposes certain limitations on this type of synthesis. However, the CVD method has established itself to be a versatile method in quality control of sample size and electrical properties. The CVD graphene grown over metals provides an adaptable form of graphene that can be transferred to desired substrates, including transparent and flexible substrates, and can be carved into various patterned circuits. The most common type is CVD graphene grown on Cu, usually polycrystalline, where grain size and disorder determine its electrical quality [21]. For applications and mass-scale studies, CVD graphene serves as a key platform, being the most viable technology that is also industry compatible. Over the past decade, this has led to significant progress in CVD graphene quality and its performance for graphene electronics and spintronics. This review aims to present a perspective on CVD graphene, where we discuss the synthesis method and the electronic and spintronic quality of CVD graphene. It is worth mentioning here that this review only focuses on selected systems to provide a perspective on CVD graphene growth, its utilization for nanoelectronic and spintronic applications (including their implementation onto flexible substrates), as well as discusses the performance of CVD graphene in terms of the ballistic transport and spin transport capabilities.

2. Overview and challenges: growth of CVD graphene

Essentially a CVD graphene growth setup consists of a furnace equipped with a temperature control unit, a quartz tube, and a rotary pump for maintaining the vacuum inside the growth chamber (quartz tube) as presented in figure 1(a). Briefly, for the graphene synthesis, a metal substrate is annealed in Ar/H_2 atmosphere at a temperature >900 °C, followed by exposure to H_2/CH_4 mixture. Here, the transition metal foil works as a catalyst and promotes graphene growth, and annealing helps to remove the residues and impurities and the increment in their grain sizes. In between the gases, H_2 creates a reducing environment in the reaction chamber and CH_4 acts as a carbon source, which decomposes over the transition metal substrate at high temperature to form the graphene film. The first report for the CVD graphene synthesis (on the Ni substrate) dates back to 2008 [22]. Followed by this, graphene CVD synthesis was reported on Ni and Cu substrates [23–26]. The growth of single layer or multilayer graphene on metal substrates strongly depends on the carbon atom solubility in that particular metal foil. Graphene growth mechanisms for the two most used metal substrates, Ni and Cu, are quite different. For Ni, due to their high solubility, carbon atoms get dissolved in the foil at higher temperatures and precipitate over the surface in the form of a film while cooling down [27]. This leads to the growth of multilayer graphene mostly on Ni substrates, and its controllability for the only single layer is also very delicate. In contrast, Cu has an ultralow solubility for carbon atoms, even if the concentration of carbon atoms is very high. So, once the reaction temperature is achieved, a hydrocarbon serving the purpose of carbon source is passed inside the reaction chamber, where it decomposes near the Cu surface and gets deposited in the form of a thin film. When the whole Cu surface is covered with decomposed carbon atoms, no further decomposition of the passing hydrocarbon occurs due to Cu's catalytic nature, limiting the growth process [28]. The first report of CVD graphene growth on Cu substrate was by Li *et al* on 25 μm thick Cu foils in a hot wall furnace [24]. In addition to Ni and Cu, several other metal substrates such as Ru [29], Ir [30], Pt [31], Fe [32], Co [33, 34], Pd [35], and Re [36], have been explored for graphene CVD synthesis. However, due to its self-limiting growth control and low cost, Cu remains the most used CVD growth substrate for graphene.

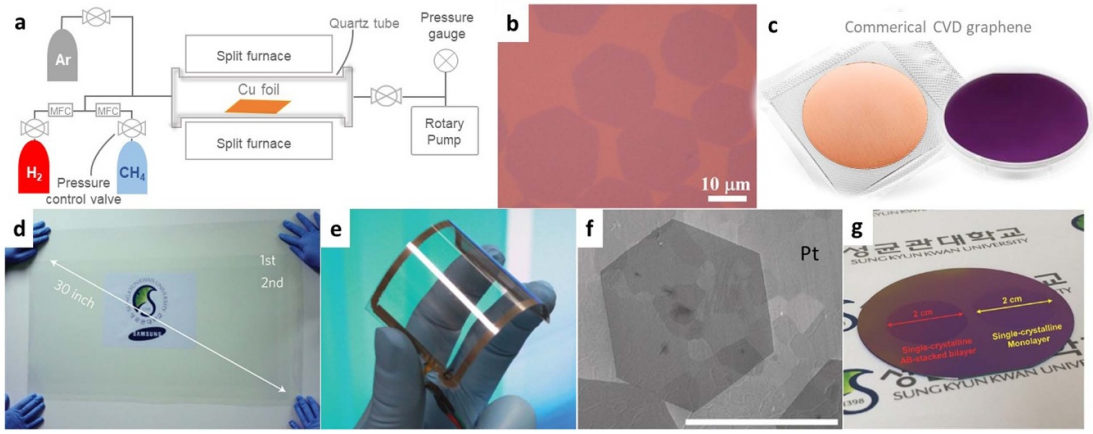

Figure 1. CVD graphene synthesis and processing. (a) Schematic showing CVD synthesis of graphene on Cu foil. (b) Typical optical images of hexagonal graphene flakes on SiO_2/Si substrate. Reproduced with permission from [53]. (c) Optical images of wafer-scale commercial graphene film (courtesy of Graphenea Inc.). (d) Transparent ultra large-area graphene film transferred on a 35-inch PET sheet. (e) Assembled graphene/PET touch panel showing outstanding flexibility. Reprinted with permission from Springer Nature Customer Service Centre GmbH: Nature, Nature Nanotechnology [54] (2010). (f) Scanning electron microscope (SEM) image of hexagonal graphene grains (scale bar is 1 mm) on a polycrystalline Pt foil, grown with 4 sccm CH_4 and 700 sccm H_2 at 1040 °C for 180 min. Reprinted with permission from Springer Nature Customer Service Centre GmbH: Nature, Nature Communications [50] (2012). (g) Photograph of single-crystalline AB-bilayer graphene and monolayer graphene of 2 cm in diameter each. [55] John Wiley & Sons. Copyright 2016 WILEY-VCH Verlag GmbH & Co. KGaA, Weinheim.

The CVD graphene film grown over Cu substrates is generally polycrystalline and consists of grains with many different orientations. These domains are pentagonal, heptagonal, and octagonal rings merging and forming line defects called graphene grain boundaries (GGBs). Recently, Fan *et al* have reported a fast and efficient method to visualize these GGBs on SiO_2/Si substrates using HF vapor exposure for different time intervals [37]. HF vapor diffuses through the GGBs and etches the SiO_2/Si to allow direct visualization of the GGBs under an optical microscope. However, these GGBs are mainly responsible for scattering the charge carriers and, thus, degrade the graphene film quality vis-à-vis their electronic applications. The growth of single-crystal graphene could be a solution to overcome this difficulty. In this regard, Ruoff's and James Tour's groups have reported millimeter-sized single-crystal graphene synthesis on Cu foils independently [38, 39].

The primary strategy to grow large-size single-crystal graphene film is by controlling the nucleation density and the orientation of different domains in their nascent stages of growth. There are several ways to manage the number of nucleates, of which modifying the substrate surface or controlling the amount of carbon precursor are two strategies. Modulation of surface characteristics of the metal surfaces could be achieved in many ways like surface rinsing, etching, polishing, and annealing. Hao *et al* treated the Cu foil surface with acetic acid for 8 h before graphene growth and reported the first-centimeter-sized graphene film [40]. In other reports, apart from acetic acid, the Cu foil surface has also been treated with $FeCl_3$, $NH_4S_2O_8$, HF, HCl, KOH, and $HNO_3$to control the nucleation density for single-crystal graphene growth [41, 42]. Besides, electrochemical polishing and chemical mechanical polishing are the two other ways to control the Cu foil surface nucleation density to grow large-sized single-crystal graphene films [43–46].
High-temperature annealing of Cu foils is also promising to control the nucleation density. Generally, high temperature, high pressure, and long duration annealing are favorable for reducing nucleation density on Cu foil surfaces [39, 47, 48]. It is worth noting that high-temperature annealing increases the Cu grain sizes, but it does not influence the graphene grain size. Exposure of Cu foil to Ar, N_2, H_2, CO_2, and O_2 during annealing also improves the reduction in nucleation density [49–51]. Epitaxial Cu (100), obtained by the melting-resolidification process, is another method to minimize the nucleation density [52].

Although the reduction in nucleation density is an effective way to synthesize large-sized single-crystal graphene film, its growth rate is painstakingly low. So, an alternative method to grow large-sized single-crystal graphene film in a comparatively fast way could be via the simultaneous growth and seamless merging of well-aligned graphene domains. The orientation of simultaneously growing graphene islands is strongly determined by the interaction and lattice matching with the underlying substrate [56]. Looking into this aspect, epitaxial growth of single-crystal graphene on different metal substrates such as Cu(111) [57], Ni(111) [58], Pt(111) [59], Au(111) [60], Ir(111) [61], Rh(111) [62], Ru(0001) [29], Ge(110) [63], Mo(110) [64], as well as alloys like CuNi [65] have been reported by different groups. Among all these, growth on Cu(111) substrates is highly favorable due to its minor lattice mismatch with graphene. However, the first

wafer-scale growth of single-crystal graphene on a silicon wafer was achieved using a hydrogen-terminated germanium buffer layer [63]. Hydrogen-terminated germanium (110) has two-fold symmetry leading to the unidirectional alignment and merging multiple seedings in a predefined orientation. Furthermore, Nguyen *et al* have reported the wafer-scale formation of artificial single-crystalline bilayer graphene via aligned transfer of two single-crystalline monolayers [55]. In addition to this, several other groups have also recently reported the wafer-scale growth of single-crystal monolayer/bilayer graphene films [55, 66–68].

Scalable CVD graphene synthesis could be achieved on different metal substrates; however, its practical electronic applications are possible only on insulating substrates. For that, the CVD-grown graphene film needs to be transferred onto a desired insulating substrate such as SiO_2/Si or sapphire glass (as shown in figure 1(b)). Today, large-scale polycrystalline graphene grown on Cu can be obtained commercially; a sample picture of commercially available CVD graphene from Graphenea has been shown in figure 1(c). In addition to rigid substrates, Bae *et al* reported a roll-to-roll production and transfer technique of the CVD graphene for flexible device applications (figures 1(d) and (e)) [54]. For high electronic quality, the growth of millimeter size large-crystals without grain boundaries (figure 1(f)) has been achieved on Pt using ambient-pressure CVD [50]. In addition, as shown in figure 1(g), wafer-scale single-crystalline graphene is achieved by dedicated CVD growth methods using single-crystal Cu(111) film on sapphire(111) substrate [55]. Dry and wet transfer are the two main transfer methods for obtaining graphene onto desired insulating substrates for electronic applications. Detailed discussion for such transfer methods is out of the scope of the present review and can be found elsewhere [69–72]. Although well investigated, these transfer methods suffer from several problems such as surface contamination and defect formation and are unsuitable for wafer-scale films. The contamination and defects during the transfer process can be circumvented if CVD graphene can be directly synthesized over insulating substrates. The first study of CVD graphene growth on dielectric substrates was reported in the year 2010 [73]. Here, direct growth of graphene onto a dielectric substrate (SiO_2/Si) was demonstrated using a single-step CVD method. Monolayer graphene was formed through the surface catalytic decomposition of carbon precursor (CH_4) on thin Cu film pre-deposited on SiO_2/Si substrate. The Cu film dewets and evaporates during or immediately after the graphene growth, resulting in a direct growth of graphene on an insulating substrate [73]. In the same year, Rümmeli *et al* reported the growth of nanographene on MgO substrate at a temperature of 325 °C [74]. Subsequent reports for the synthesis of graphene using CVD on different insulating substrates, including growth over SiO_2/Si, Si_3N_4, h-BN, glass, fused silica, quartz, etc, with sizes ranging from few nanometers to several millimeters have been reported [75–94].

Overall, the developments suggest the significant progress made in the growth of CVD graphene onto various metal substrates, large-grain CVD graphene growth on specific metal substrates, as well growth on insulating substrates. Despite these advancements, the most applied systems have been CVD graphene over Cu substrate transferred onto the desired substrates. Nowadays, several companies like Graphenea, 2DTech, AdNano Technology, Advanced Graphene Products, AMO GmBH, Grafentek, Grolltex Inc. etc, are providing well-controlled mono/multilayer graphene films for industrial applications. Towards wafer-scale transfer of graphene film, in the year 2012, Gao *et al* reported the millimeter-sized synthesis of single-crystal CVD graphene film on Pt substrate (figure 1(f)) and transferred that onto a desired insulating substrate using the bubbling transfer method [50]. However, large-grain CVD graphene grown on Pt substrates is yet to be commercially viable. At the same time, despite reports of growth on insulating substrates, direct growth of high-quality graphene film over an insulating substrate remains a challenge and a possible avenue for improvement that can better integrate graphene into semiconductor fabrication technologies for device applications. In this context, singe crystal CVD graphene growth at wafer-scale on hydrogen-terminated germanium shows promise [63]. For flexible applications, the CVD graphene roll-to-roll direct transfer technique of the CVD graphene [54] and recently reported direct lamination of CVD graphene onto flexible polyethylene napthalate (PEN) substrates [95] appear promising transfer methods to obtain CVD graphene films that can have high value for industrial applications.

3. High-quality electrical transport in CVD graphene

The lack of bandgap in graphene does not make it suitable for digital switches, although nanoribbons of graphene [96–99] and the unique electronic properties of graphene reveal its augmentative potential for engineering device components and their performance in microelectronics. It is also considered an alternative for the 'More than Moore' technology [100–105] and the cornerstone of the fast-growing field of mixed-dimensional van der Waals heterostructures [106, 107]. Moreover, because it is an atomically thin electron gas directly exposed to its environment, graphene is an ideal material for sensing applications combining ultimate sensitivity with high-quality charge transport figures of merit. Hence, graphene can be combined with other nanomaterials, which can respond to multiple stimuli (pressure, temperature, light,

electric field) to create a wide variety of novel device concepts ranging from molecular electronics [108–112], switchtronics [113–116], spintronics [117–119], nanoelectronics [120–126], to optoelectronics [127–132]. However, there are challenges to obtaining the reliable quality and coverage of CVD graphene reproducibly for all these applications. The difficulties lie in controlling grain boundaries, metal contamination during growth and transfer, doping and strain during transfer processes on substrates, and contact resistance, which pose hurdles for the reliable integration of graphene to CMOS process lines. The prospects and challenges of graphene for microelectronics are dealt with in earlier reviews [133, 134]. On the other hand, graphene, in general, provides a readily available single-atomic thin material with high carrier mobility, much higher than silicon, that makes graphene suitable for high-quality electrical transport and long-distance ballistic circuits. Graphene obtained by mechanical cleavage on SiO_2/Si substrate can exhibit charge mobility up to 10 000 $cm^2\ V^{-1}\ s^1$ [2]. Considering a typical carrier concentration $\sim 10^{12}\ cm^{-2}$, such quality translates to a mean free path of the order of 100 nm. Further, it has been reported that if extrinsic scattering in graphene is eliminated, its mobility can reach ~200 000 $cm^2\ V^{-1}\ s^{-1}$ at room temperature due to weak electron-phonon coupling [135]. Experimentally, for a carrier concentration of $\sim 10^{11}\ cm^{-2}$, the mobility of graphene exceeds 100 000 $cm^2\ V^{-1}\ s^{-1}$ and 1000 000 $cm^2\ V^{-1}\ s^{-1}$ at room and liquid helium temperature, respectively [136–138]. However, all the above reports are for mechanically exfoliated graphene flakes, suitable for basic device research but not for large-scale applications. In contrast, CVD graphene has proven its potential for large-scale synthesis and scalable, practical device applications. Charge mobility in CVD graphene strongly depends upon the transfer technique, type of substrate, and environment. Mainly either polymer-supported wet transfer or dry transfer methods are used for graphene transfer [69–72]. Carrier mobility in the polymer-assisted transfer of graphene on the SiO_2/Si substrate can exceed 7000 $cm^2\ V^{-1}\ s^{-1}$ [139] at room temperature, whereas mobility up to 37 000 $cm^2\ V^{-1}\ s^{-1}$ can be obtained on an h-BN substrate at 4.2 K [140]. Further improvement in the charge carrier mobility has been reported using h-BN encapsulation and semi-dry transfer method on SiO_2/Si substrate at low temperatures [141]. The dry transfer method (figures 2(a) and (b)) provides the advantage of a clean interface and better carrier mobility of CVD graphene. Banszerus *et al* have reported a maximum of 130 000 $cm^2\ V^{-1}\ s^{-1}$ charge mobility for a van der Waals dry transferred CVD graphene at 1.8 K (figure 2) [10]. Due to such high charge carrier mobility, ballistic transport in CVD graphene has been identified using negative bend resistance for electrons and holes and mean free path along the dashed arrow in figure 2(c) as a function of charge carrier density for temperature ranging from 1.8 to 200 K (figures 2(d) and (e)). Another approach called roll-to-roll transfer for CVD graphene has been adopted by Bae *et al*, where a thermal releasing tape has been used for graphene transfer and used for flexible device applications [54]. Implementing similar transfer approach, a maximum of 8000 $cm^2\ V^{-1}\ s^{-1}$ charge mobility has been reported for CVD graphene on SiO_2/Si substrate [142]. In state-of-the-art, most commercially available CVD graphene possesses charge carrier mobility in the range of 2000–4000 $cm^2\ V^{-1}\ s^{-1}$.

The electrical properties of graphene can be affected by grain boundaries, atmospheric doping, and encapsulation effect [143]. As per available reports, the small graphene grain size shows lower average mobility, and the surface adsorption of air molecules decreases the carrier mobility in CVD graphene. In the year 2011, Mayorov *et al.* reported micrometer-scale (~1 μm) ballistic transport in hexagonal boron nitride (h-BN) encapsulated graphene at room temperature [9]. Robust transport with a significant negative value of transfer resistance and mean free path exceeding up to 3 μm (at low temperature) has been observed in h-BN encapsulated graphene devices with a mobility value ~500 000 $cm^2\ V^{-1}\ s^{-1}$. Subsequently, Banszerus *et al* have shown ballistic transport in h-BN encapsulated CVD graphene beyond ~28 μm [10]. The ballistic transport was determined by measuring the negative bend resistance ($R_B = V_B/I$) in cross and square-shaped CVD graphene devices. With a distinct minimum in the electron regime close to the charge neutrality point, the bend resistance was found negative for both electrons as well as holes at low temperatures. The bend resistance exhibits an assertive temperature-dependent behavior and becomes positive for all kinds of charge carriers above 200 K, confirming the transition to the diffusive charge transport regime. Recently, high mobility up to ~70 000 $cm^2\ V^{-1}\ s^{-1}$ and ~120 000 $cm^2\ V^{-1}\ s^{-1}$ at room temperature and at 9 K have also been demonstrated for wet transferred single-crystal monolayer graphene [72], where ballistic transport over ~600 nm has been observed. Using a similar approach for polycrystalline graphene film, the achieved mobility exceeds ~7000 $cm^2\ V^{-1}\ s^{-1}$ at room temperature and up to ~30 000 $cm^2\ V^{-1}\ s^{-1}$ after annealing in Ar/H_2 environment at 600 °C. Along with these, other similar reports have been listed in table 1. In the year 2006, Tőke *et al* theoretically predicted the existence of fractional quantum Hall effect in graphene [144], and in the year 2009, two research groups reported the experimental observation of fractional quantum Hall effect in suspended graphene samples [5, 145]. Schmitz *et al* have recently shown the emergence of fractional quantum Hall states in dry transferred high-quality CVD graphene in magnetic fields from below 3 T to 35 T, comparable to exfoliated graphene [6]. Furthermore, they observed the effective composite-fermion filling factor up to $\nu^* = 4$ with higher-order composite-fermion states at higher

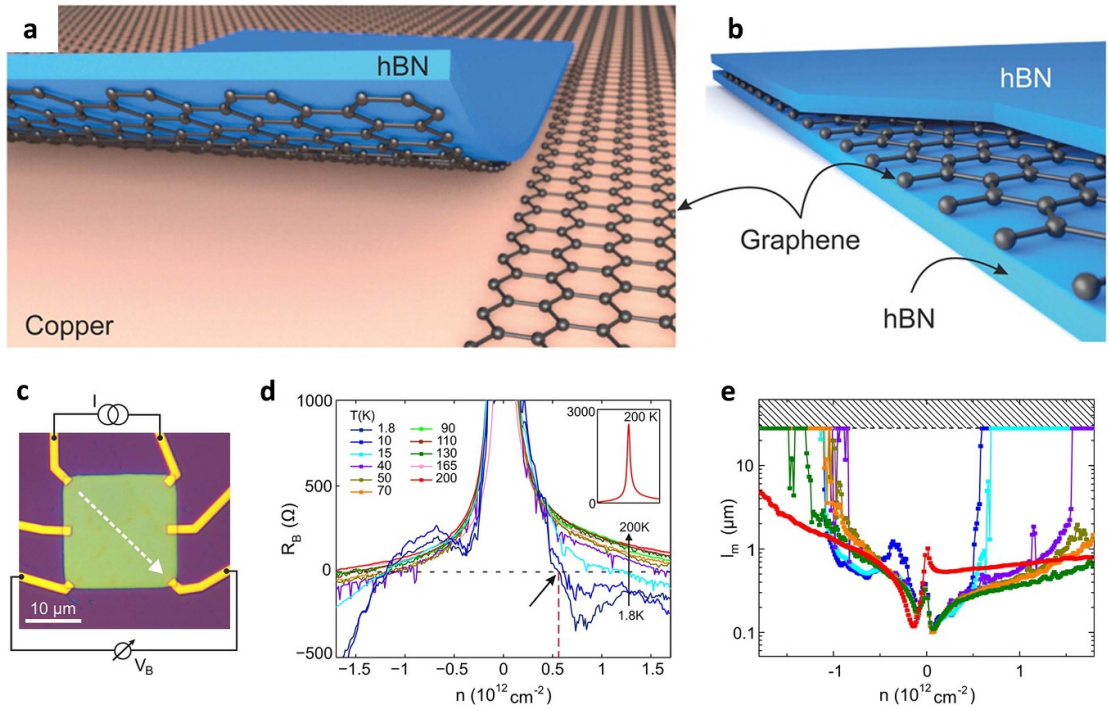

Figure 2. Ballistic transport in high-quality CVD graphene. (a) Illustration for graphene delamination from copper foil by van der Waals pick-up by h-BN. The graphene sheet is stamped out along the edges of the h-BN flake. (b) The h-BN/graphene flake is placed on another h-BN flake resulting in a sandwiched structure. (c) Optical image of h-BN/graphene/h-BN device with Cr/Au side contacts. The arrow shows the direction of the ballistic transport measurement length (∼28 μm). (d) Bend resistance as a function of charge carrier concentration for temperature ranging from 1.8 to 200 K. The inset shows fully diffusive charge transport of complete R_B at 200 K. (e) Elastic mean free path calculated from selected R_B traces. Reprinted with permission from [10]. Copyright (2016) American Chemical Society.

magnetic fields. Concurrently Pezzini *et al* reported high-mobility encapsulated CVD graphene devices showing the onset of Landau quantization (magnetic fields ∼50 mT), electronic correlation, and signatures of fractional quantum Hall effect [141]. A list of high-quality CVD graphene charge-based devices with observed key charge transport parameters is summarized in table 1. Overall, considering the versatility of h-BN in electrical, optical, and photonic applications and the progress in synthesis techniques of large-grain h-BN and its heterostructures [146, 147], these reports of ballistic and quantum transport features show promise of high-quality CVD graphene for new nanoelectronic and metrology sensors.

3.1. CVD graphene flexible electronic devices

Beyond a high-mobility system, graphene's outstanding mechanical strength and flexibility due to its atomically thin structure make it a key frontline material for multiple flexible electronic device applications, and here we provide some illustrative examples. CVD graphene has been employed to demonstrate various kinds of devices ranging from field-effect transistors (FETs) to radio-frequency circuits, graphene terahertz detectors, and flexible Hall sensors. Kim *et al* have demonstrated high-performance, low voltage (<3 V) flexible CVD graphene FET arrays with a high capacitive ion-gel dielectric. The CVD graphene FETs fabricated on PET substrate showed mobility of 203 ± 57 and 91 ± 50 $cm^2\,V^{-1}s^{-1}$ for holes and electrons, respectively [148]. Lu *et al* have fabricated CVD graphene FET arrays on flexible plastic substrate using natural Al_2O_3 as dielectric [149]. The use of Al_2O_3 as dielectric brought several advantages like high capacitance, self-alignment, minimum resistance, and a good on/off ratio at a low operational voltage (<3 V) along with high mobility up to 230 and 300 $cm^2\,V^{-1}s^{-1}$ for electrons and holes, respectively. In addition, the use of aluminum oxide dielectric is also seen to cause self-healing of the device upon electrical breakdown. On the other hand, high mobility CVD graphene transistors fabricated over flexible polyimide substrates have shown maximum carrier mobility of 3900 $cm^2\,V^{-1}s^{-1}$ with 25 GHz cut-off frequency, which was ∼3 times larger than prior reports [150], with 2–5 times improved flexibility than the earlier reports. CVD graphene flexible FETs capable of working under modest strain have been fabricated on PEN polymer substrates [151]. These FETs have not only shown carrier mobilities of 13 540 and 12 300 $cm^2\,V^{-1}s^{-1}$ for holes and electrons, respectively, but also a high current density of 200 μA μm^{-1} with saturation, and a perfect ambipolar electron–hole behavior with a good transconductance of 120 μS μm^{-1} [151]. Using CVD graphene, terahertz detectors with a voltage responsivity above 2 V W^{-1} and estimated noise equivalent

Table 1. Summary of high-quality charge and spin transport results in CVD graphene showing ballistic transport (ballistic mean free path λ_{mfp}) and spin transport parameters (spin diffusion length λ_{sd}, spin lifetime τ). Unless specifically mentioned, the mobility values indicate electron mobility.

	System		Reference	Mobility ($cm^2\ V^{-1}\ s^{-1}$)	Temperature (K)	τ (ns)	λ (μm)
Ballistic transport	CVD graphene dry transferred onto h-BN flakes		[192]	$\mu_h = 42\,000$ $\mu_e = 29\,000$	4	—	$\lambda_{mfp} = 1$
	CVD bilayer graphene-h-BN heterostructure		[193]	180 000 40 000	2 300	—	$\lambda_{mfp} = 2$
	h-BN encapsulated single-layer CVD graphene		[72]	70 000 120 000	300 9	—	$\lambda_{mfp} = 0.6$ $\lambda_{mfp} = 1$
	CVD graphene/h-BN heterostructure		[194]	$\mu_h = 350\,000$ $\mu_e = 320\,000$	1.6	—	—
	CVD graphene encapsulated in h-BN		[10]	147 000	1.8–300		$\lambda_{mfp} = 1$–28
Spin transport	**CVD graphene**	h-BN-stack	[195, 196]	21 000 20 000 (FLG)	300 300	12.6 3.7	$\lambda_{sd} = 30.5$ $\lambda_{sd} = 10$
		Co/TiO_2	[180]	2000–3000	300	3.46	$\lambda_{sd} = 13.6$
		Co/MgO	[168]	1 400 (SLG) 2 100 (BLG)	5–300	0.180 (SLG) 0.285 (BLG)	$\lambda_{sd} = 1.1$ (SLG) $\lambda_{sd} = 1.35$ (BLG)
		Co/TiO_2	[175]	2000	4.2–300	1.2	$\lambda_{sd} = 6$
		Co/TiO_2	[197]	2000	300	0.405	$\lambda_{sd} = 3.4$
		Co/TiO_2	[185]	1700	300	3	$\lambda_{sd} = 9.2$
		Co/h-BN	[198]	850	4.2–300	0.260	$\lambda_{sd} = 1.2$
		Co/h-BN	[199]	3400	300	0.404	$\lambda_{sd} = 3.5$
		Co/MgO/h-BN	[200]	20 000	300	1.75	$\lambda_{sd} = 4.3$

power below 3 nW/√Hz have also been demonstrated by Yang *et al* [152]. CVD graphene-based flexible Hall sensors with voltage and current sensitivities up to 0.096 V VT^{-1} and 79 V AT^{-1} have also been realized. Such sensors showed robustness to a minimum bending radius up to 4 mm (corresponding to a tensile strain ∼0.6%) and 1000 bending cycles [153]. Furthermore, Uzlu *et al* have used flexible CVD graphene-based Hall sensors on polyimide substrates for significant increment in the signal to noise ratio compared to Hall sensors working with static operations, and the minimal detectable magnetic field goes down to 290 nT/√Hz with a sensitivity up to 0.55 V VT^{-1} [154].

Overall, the charge transport investigations in CVD graphene have shown exciting results from observing quantum Hall and fractional quantum Hall effects to high-mobility h-BN-based heterostructures that enable micron-scale ballistic transport. These reports suggest that CVD graphene is a medium to harness the unique quantum transport and ballistic transport properties for developing dedicated sensing and new conceptual advancement in nanoelectronics and metrology. In addition, charge transport CVD graphene devices of regular quality show prospects in developing flexible circuits with significant opportunities for flexible multipurpose nanoelectronic circuits. However, at the same time, challenges exist in large-scale implementation of such systems reproducibly and reliably, which would require advancements in direct growth or transfer technologies for high-quality heterostructures.

4. Progress in long distance spin transport in CVD graphene

The present-day spintronic applications such as magnetic memory and magnetoresistive random-access memory have emerged from the giant and tunnel magnetoresistance effects [155] and spin-transfer torque effects [156]. Beyond such applications in basic layered structures of ferromagnet–nonmagnet–ferromagnet (FM–NM–FM) stack, advanced multi-terminal planar devices operating with spin currents for computing and sensing are also possible if lateral spin transport can be achieved over long distances. Lateral metal spintronics showed promise in this direction [157]; however, the low spin diffusion lengths in metals at room temperature hinder it. Here, graphene brought fresh inspiration to spintronics due to its spin transport capability. Owing to its low spin–orbit coupling (light C-12 atoms) and negligible hyperfine interaction, long spin diffusion length $\lambda \sim 100\ \mu$m, and high spin lifetime $\tau \sim 1\ \mu$s have been theoretically predicted [11] in graphene, which led to its initial experimental investigations into spin injection and spin valve devices [12, 158–160]. In 2007, the first experimental demonstration using non-local measurement technique in graphene revealed spin transport as well as precession across channel length ∼2 μm (shown in figure 3(a)), surpassing such capability of any other material (where spins travel ∼100 nm) at room temperature [12]. As shown for a graphene device in figure 3(b), electrical current I from injector magnetic electrode into graphene causes spin accumulation in graphene and pure spin currents detected by a voltage drop by non-local detector voltage circuit. The current circuit I causes electrical spin injection into graphene, creating a difference in the chemical potentials of spin up ($\mu_\uparrow$) and spin down ($\mu_\downarrow$) electrons, which diffuse through graphene. The isolated voltage circuit (V) measures pure spin transport signal by the separate contacts placed at a distance L. The spin accumulation $\Delta\mu = \mu_\uparrow - \mu_\downarrow$ is measured by the voltage difference $\Delta V_{\mathrm{NL}} = V_{\uparrow\uparrow} - V_{\uparrow\downarrow}$ obtained by switching the magnetic orientation of the injector (I) and detector (D) from parallel (↑↑ or ↓↓) to antiparallel (↓↑ or ↑↓), achieved by sweeping an in-plane magnetic field ($\boldsymbol{B}_\parallel$). Such measurement is called spin-valve measurement and $R_{\mathrm{NL}} = V_{\mathrm{NL}}/I$ is called the non-local resistance. In another measurement geometry, called the Hanle measurement technique, by keeping the injector-detector parallel or antiparallel, an out-of-plane magnetic field ($\boldsymbol{B}_\perp$) is swept to get continuous variation in spin signal due to Larmor spin precession with frequency $\omega_{\mathrm{L}} = \frac{g\mu_{\mathrm{B}}}{\hbar} B_\perp$ (where g, μ_{B}, and $\hbar$ are standard constants). Analysis of the Hanle signal gives spin lifetime τ, diffusion constant D, and diffusion length λ. This method pioneered by Johnson and Silsbee [161] is a reliable method of isolating charge and spin currents for pure spin transport measurements in metals, semiconductors, and graphene. In contrast to local two-terminal measurement of magnetoresistance of an FM–NM–FM junction, this method avoids other magnetoresistance sources such as ordinary and anisotropic magnetoresistances of the component materials.

The demonstration of spin transport and precession by Tombros *et al* [12] propelled research in graphene spintronics, with initial reported spin diffusion length $\lambda \sim 1.5\ \mu$m and spin lifetime $\tau \sim 150$ ps consistently improved by experimentalists chasing the theoretically predicted values. Improvements in spin transport are possible with good (a) quality of ferromagnetic contacts on graphene and (b) quality of graphene channel. In the context of (a), tunnel spin injection using metal oxide barriers showed enhancement in spin injection [162], yielding better spin parameters. This includes improvements in tunnel spin injection into graphene using atomically thin hexagonal boron nitride (h-BN) tunnel barriers [163, 164] as a novel alternative to oxide barriers. In contrast, for (b), graphene over h-BN atomically flat substrates and graphene encapsulated between h-BN heterostructures revealed high-quality graphene channel, with reported values of spin diffusion length $\lambda \sim 12\ \mu$m and $\tau \sim 2$ ns at room temperature [165]. However, most

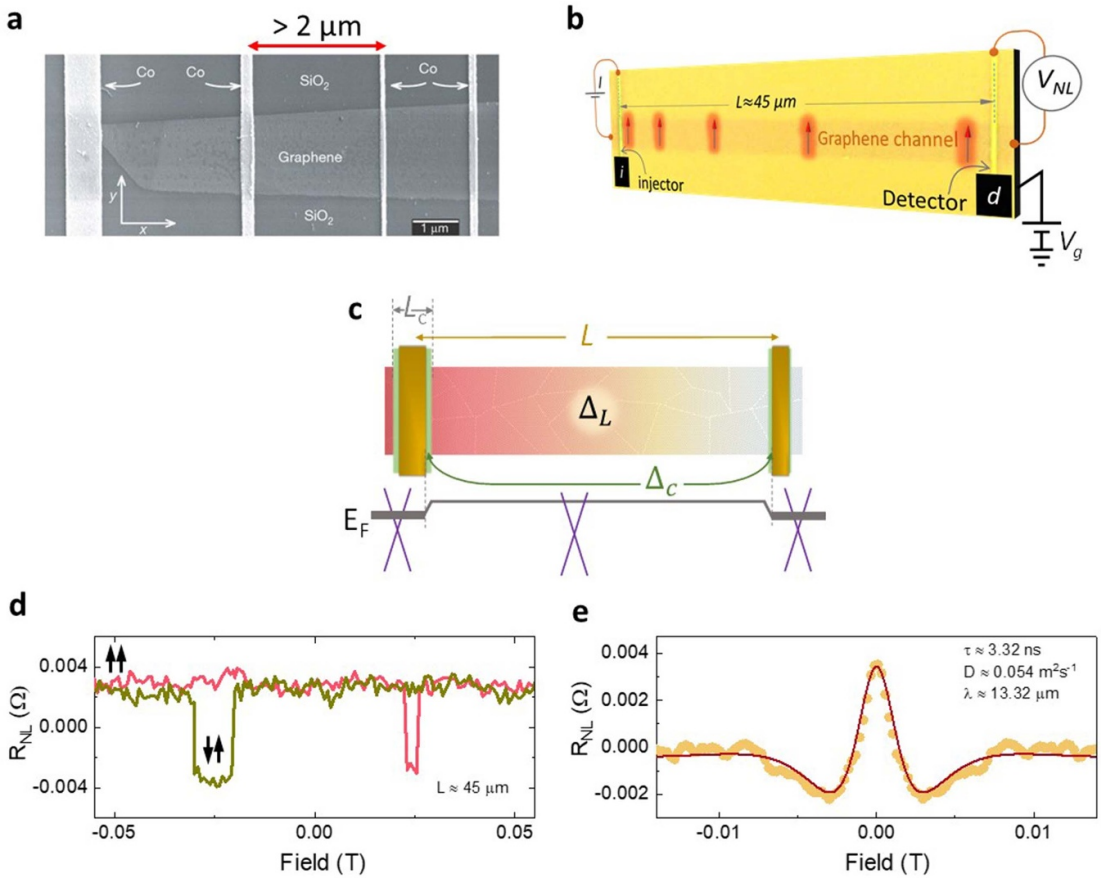

Figure 3. Extremely long spin transport in graphene. (a) Exfoliated graphene device with multiple contacts used by Tombros *et al.* Reprinted with permission from Springer Nature Customer Service Centre GmbH: Nature, Nature [12] (2007). (b) State-of-the-art longest (45 μm) spin transport graphene device with nonlocal measurement configuration. (c) Scheme showing spin diffusion in graphene by the fading red color and doping profile across the device. Δ_L and Δ_C indicate the spin–orbit coupling in the channel and contact regions, respectively. Experimentally observed (d) spin valve and (e) spin precession Hanle measurement data fit with extracted spin parameters. (b)–(e) Reproduced from [180]. CC BY 4.0.

of these studies focused on exfoliated single crystals, which were preferred to polycrystalline CVD graphene, as the latter featured grain boundaries and defects and accumulated impurities and ripples during the fabrication process. Despite enhancements using special encapsulated structures [166] and some exceptions [162], routine devices still show $\lambda \sim 1.5$ μm and $\tau \sim 150$–200 ps for graphene on widely used substrates such as oxidized silicon wafers [167]. Similar spin parameters were also observed in the earliest studies performed using wafer-scale CVD graphene [168]. The inherent spin relaxation in graphene occurs via Elliot-Yafet (EY) relaxation [169] and D'yakonov-Perel' (DP) mechanisms [170] that yield theoretical values of τ in the μs range [11, 169, 171]. Experiments of spin transport in graphene showing $\tau \sim 0.5$–1 ns attributed the quantitative effects to EY [172] and both mechanisms [173–175]. Besides, specific mechanisms such as spin-pseudospin entanglement in quasi-ballistic transport regime [176, 177] and scattering due to magnetic moments, vacancies, and defects [178, 179] also match experimental spin lifetimes ~few 100 ps.

Polycrystalline CVD graphene grown over Cu substrates features grain sizes of the order of a few 100 nm to a few microns [181, 182]. Despite this, theory suggests that in such a form of graphene, ripples or wrinkles [183, 184], corrugations and flexural distortions [184] do not set the lower limit of τ, which makes CVD graphene a promising platform for spintronic investigations. In 2015, the demonstration of long-distance spin communication in CVD graphene over distances ~16 μm with high spin diffusion length $\lambda \sim 6$ μm and spin lifetime $\tau \sim 1.2$ ns at room temperature [175], showed promise of the large form of graphene for exploration for scalability and applications. Another key report showed improved performance with $\lambda \sim 7$–9 μm and $\tau \sim 2$–3 ns in channel lengths ~30 μm, enabled in CVD graphene grown over Pt substrate, which is considered favorable for large-grain sized graphene [185]. Although large grains reduce grain boundary scattering that could result in enhanced spin lifetimes, recent theoretical predictions suggest grain size independence of spin diffusion length in graphene [186]. This has been observed in recently performed experiments in polycrystalline commercial CVD graphene, that showed the highest performance $\lambda \sim 13.6$ μm and $\tau \sim 3.5$ ns observed in longest spin communication graphene channels ~45 μm

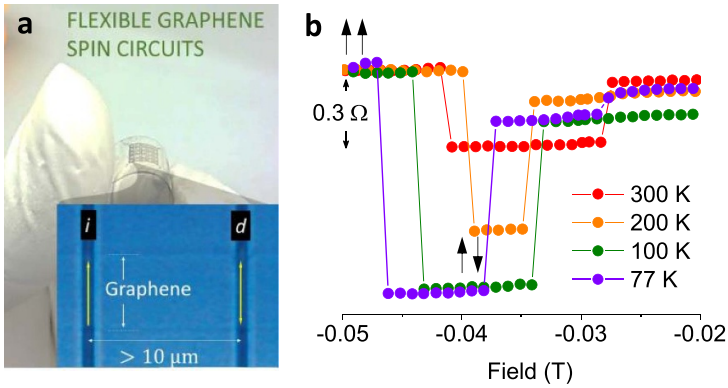

Figure 4. Spin transport in graphene on flexible substrates. (a) Arrays of graphene devices on flexible PEN substrate. Inset: optical micrograph of a single device with magnetic injector and detector contacts on graphene. (b) Spin valve switching obtained by switching between parallel and anti-parallel configuration of the injector-detector contacts. Adapted with permission from [190]. Copyright (2019) American Chemical Society.

(figures 3(b)–(e)), including robust spin transport under ambient conditions [180]. The observations on multiple extremely long channels 10–45 μm, suggest that the longest channels reduce the impact of contact-induced surface charge transfer doping regions and device doping, that results in enhanced $\lambda \sim 13.6$ μm corresponding to $\Delta_{SOC} \sim 20$ μeV expected for graphene over SiO_2/Si with D'yakonov-Perel' (DP) dominant mechanism [180]. A list of CVD graphene-based spin devices with observed spin parameters is presented in table 1.

4.1. Towards flexible graphene spintronics

While these bring the promise of practically applicable graphene systems, graphene is also known for its outstanding resilience, making it ideal for flexible nanoelectronics. The realization of spin transport in graphene on flexible substrates is the first step towards enabling flexible graphene spintronics. One key hurdle here is the roughness associated with flexible substrates, extending up to several nm, compared to the roughness ~0.3 nm of SiO_2/Si. On the other hand, for efficient graphene spintronic devices, atomically flat substrates such as heterostructures of graphene on atomically flat boron nitride substrates [165, 166] have been seen to improve spin transport by avoiding roughness-induced carrier scattering. However, the nanometric roughnesses of flexible substrates are expected to introduce curvature-induced spin–orbit coupling [187, 188] in graphene. Furthermore, CVD graphene on flexible substrates, possessing large surface roughness compared to conventional silicon wafers, can show modified Fermi velocities [189]. In addition, the stability of ferromagnetic contacts onto graphene in spin devices is also a concern. Despite these and other experimental challenges both in fabrication and measurements, spin transport in CVD graphene over large-scale flexible PEN substrates was demonstrated in 2019 [190] (figure 4). The ferromagnetic nanowires in such systems have been found to be resilient due to ultralow magnetostriction [191]. Additionally, the graphene spin devices fabricated on PEN substrates showed consistently robust spin signals with channel lengths extending up to 15 μm at room temperature. Here, despite moderate spin lifetimes $\tau \sim 0.25$–39 ns, relatively large spin diffusion lengths $\lambda \sim 8$–10 μm, attributed to high spin diffusion coefficient ~0.2 $m^2 s^{-1,}$ were obtained. Although counterintuitive, and despite the nanometer level roughness of polyethylene-based substrates, atomic force microscopy reveals topography with minor intra-peak roughness of PEN ($\leqslant$1 nm), which suggests reduced roughness scattering for improved charge as well as spin diffusion through graphene over PEN. This demonstration provides a path for exploring and integrating graphene spin valves into flexible and transparent nanoelectronic devices.

The past decade's investigations cemented the prospect of CVD graphene for spin transport and obtaining spin currents over long distances, even under ambient conditions [180]. With the relatively cheap availability of commercial CVD graphene, despite its polycrystallinity, it emerges as a robust large-scale promising material for exploring spin currents, not only for fundamental research but also for their applicability in lateral spin sensors and research and development exploration of the practical application of graphene spintronics. While spin current exploration could be further directed beyond CMOS spin-logic integrated architectures, a short-term prospect would be to explore the industrial investigation of graphene for position, velocity, or angle-sensing spintronic applications and their implementation into flexible electronics. In addition to planar transport, graphene|ferromagnetic interfaces are considered to show several exciting spin filtering properties and voltage-controlled polarization [201, 202]. Since CVD graphene can be

readily grown on ferromagnetic metals such as Ni, it has emerged as a new system for spinterface phenomena [203]. The graphene layer passivates the ferromagnetic thin film used for the CVD growth and provides a protected spin-polarized electrode compatible with standard lithography processes and resistant to solvents or water [204–207]. Such graphene|ferromagnetic interfaces are attractive means to develop organic spintronic and magneto-Coulombic devices [123]. These unique properties constitute a dedicated avenue that has been dealt with in a recent review on 2D spinterfaces and magnetic interfaces [203]. Additionally, recent works have revealed that the spin transport mechanisms and spin-polarized energy landscapes can be tailored upon modifying the interface interaction/hybridization, opening new prospects for spinterfaces with increased performances and novel functionalities [208, 209].

5. Summary and future perspective

Over the past decade, significant progress has been made in CVD graphene growth on different substrates, large-size crystals controlled by growth conditions, including the possibility of wafer-scale single crystals as processing methods for good quality samples. Such a form of graphene has been proved to be of practical value for electronic and spintronic devices and their implementation onto flexible substrates. Of unique importance is the electrical mobility of CVD graphene crystals, which can be enhanced by high-quality encapsulated heterostructures, leading to the observation of ballistic transport over tens of micrometers, fractional quantum Hall effect, and composite-fermions. In the context of spin transport, today, even commercial CVD graphene shows extremely long spin communication capabilities with spin diffusion lengths surpassing 10 μm, and robust performance under ambient conditions. In addition to CVD graphene, significant progress has also been made in other 2D materials at relatively low temperatures (<500 °C) [210], in particular transition metal dichalcogenides [211]. When combined with CVD graphene, such large-scale two-dimensional quantum materials [212] allow for the practical exploitation of magnetic, topological, or spin–orbit proximity effects that can be engineered by van der Waals heterostructures [213] for developing novel technologies using CVD graphene. These prospects and developments make CVD graphene a promising platform for nanoelectronic circuits, spin circuits, flexible devices, and quantum metrology applications. At the same time, challenges exist in achieving high reliability in mass fabricated CVD graphene devices and their implementation into microelectronics [133, 134]. The correlation between sample sheet resistance and grain size is a critical issue in commercial CVD graphene [21, 214], where essentially polycrystallinity leads to varying electronic quality in batch to batch prepared wafers. The throughput does not seem practical for scalability in single-crystalline and high electronic quality samples prepared by dry transfer techniques. Here, reports showing wafer-scale single-crystalline graphene, industry compatible processing methods [215], and lamination techniques [95] show promise for improvements and implementation on a large scale to tackle such challenges. A promise comes from the fact that CVD is a method employed in microelectronics to deposit conformal thin films of materials. If CVD graphene growth technologies of direct-deposition onto circuitry are realized, CVD graphene can be combined to semiconductor fabrication lines. The requirements would be optimization in fabrication technologies, contact engineering, and packaging for consistently obtaining high throughput performance and high reliability. With continuous progress and standardization in high-quality devices, growth, processing, and integration technologies, there is a true scope for fully harnessing graphene's unique quantum and spin transport attributes for future novel electronic and spintronic applications.

Data availability statement

No new data were created or analysed in this study.

Acknowledgments

We acknowledge funding from Swedish Research Council (VR starting Grant Nos. 2016–03278 and 2017–05030), Carl Tryggers Stiftelse för Vetenskaplig Forskning (Grant No. CTS 18:271), Stiftelsen Olle Engkvist Byggmästare (200–0602), Energimyndigheten (48698–1), Formas (Grant No. 2019–01326), and Wenner-Gren Stiftelserna (UPD2018-0057, UPD2018-0003, and UPD2019–0166). J-F D thanks the Institut Universitaire de France (IUF) and the Agence Nationale de la Recherche (MIXES ANR-19-CE09-0028) for financial support.

ORCID iDs

T Sarkar https://orcid.org/0000-0003-4754-2504
J-F Dayen https://orcid.org/0000-0001-5625-9263
M Venkata Kamalakar https://orcid.org/0000-0003-2385-9267

References

[1] Novoselov K S, Geim A K, Morozov S V, Jiang D, Zhang Y, Dubonos S V, Grigorieva I V and Firsov A A 2004 Electric field effect in atomically thin carbon films *Science* **306** 666–9
[2] Geim A K and Novoselov K S 2007 The rise of graphene *Nat. Mater.* **6** 183–91
[3] Wallace P R 1947 The band theory of graphite *Phys. Rev.* **71** 622–34
[4] Novoselov K S, Geim A K, Morozov S V, Jiang D, Katsnelson M I, Grigorieva I V, Dubonos S V and Firsov A A 2005 Two-dimensional gas of massless dirac fermions in graphene *Nature* **438** 197–200
[5] Bolotin K I, Ghahari F, Shulman M D, Stormer H L and Kim P 2009 Observation of the fractional quantum Hall effect in graphene *Nature* **462** 196–9
[6] Schmitz M, Ouaj T, Winter Z, Rubi K, Watanabe K, Taniguchi T, Zeitler U, Beschoten B and Stampfer C 2020 Fractional quantum Hall effect in CVD-grown graphene *2D Mater.* **7** 041007
[7] Katsnelson M I, Novoselov K S and Geim A K 2006 Chiral tunnelling and the Klein paradox in graphene *Nat. Phys.* **2** 620–5
[8] Mishchenko E G 2008 Minimal conductivity in graphene: interaction corrections and ultraviolet anomaly *EPL* **83** 17005
[9] Mayorov A S *et al* 2011 Micrometer-scale ballistic transport in encapsulated graphene at room temperature *Nano Lett.* **11** 2396–9
[10] Banszerus L, Schmitz M, Engels S, Goldsche M, Watanabe K, Taniguchi T, Beschoten B and Stampfer C 2016 Ballistic transport exceeding 28 μm in CVD grown graphene *Nano Lett.* **16** 1387–91
[11] Huertas-Hernando D, Guinea F and Brataas A 2006 Spin-orbit coupling in curved graphene, fullerenes, nanotubes, and nanotube caps *Phys. Rev.* B **74** 155426
[12] Tombros N, Jozsa C, Popinciuc M, Jonkman H T and Van Wees B J 2007 Electronic spin transport and spin precession in single graphene layers at room temperature *Nature* **448** 571–4
[13] Avsar A, Ochoa H, Guinea F, Özyilmaz B, Van Wees B J and Vera-Marun I J 2020 Colloquium : spintronics in graphene and other two-dimensional materials *Rev. Mod. Phys.* **92** 021003
[14] Choi W, Lahiri I, Seelaboyina R and Kang Y S 2010 Synthesis of graphene and its applications: a review *Crit. Rev. Solid State Mater. Sci.* **35** 52–71
[15] Zhang Y, Zhang L and Zhou C 2013 Review of chemical vapor deposition of graphene and related applications *Acc. Chem. Res.* **46** 2329–39
[16] Muñoz R and Gómez-Aleixandre C 2013 Review of CVD synthesis of graphene *Chem. Vap. Depos.* **19** 297–322
[17] Rollings E, Gweon G H, Zhou S Y, Mun B S, McChesney J L, Hussain B S, Fedorov A V, First P N, De Heer W A and Lanzara A 2006 Synthesis and characterization of atomically thin graphite films on a silicon carbide substrate *J. Phys. Chem. Solids* **67** 2172–7
[18] De Heer W A *et al* 2007 Epitaxial graphene *Solid State Commun.* **143** 92–100
[19] Tedesco J L, VanMil B L, Myers-Ward R L, McCrate J M, Kitt S A, Campbell P M, Jernigan G G, Culbertson J C, Eddy C R and Gaskill D K 2009 Hall effect mobility of epitaxial graphene grown on silicon carbide *Appl. Phys. Lett.* **95** 122102
[20] Grodecki K, Blaszczyk J A, Strupinski W, Wysmolek A, Stępniewski R, Drabinska A, Sochacki M, Dominiak A and Baranowski J M 2012 Pinned and unpinned epitaxial graphene layers on SiC studied by Raman spectroscopy *J. Appl. Phys.* **111** 114307
[21] Cummings A W, Duong D L, Nguyen V L, Van Tuan D, Kotakoski J, Barrios Vargas J E, Lee Y H and Roche S 2014 Charge transport in polycrystalline graphene: challenges and opportunities *Adv. Mater.* **26** 5079–94
[22] Yu Q, Lian J, Siriponglert S, Li H, Chen Y P and Pei -S-S 2008 Graphene segregated on Ni surfaces and transferred to insulators *Appl. Phys. Lett.* **93** 113103
[23] De Arco L G, Zhang Y, Kumar A and Zhou C 2009 Synthesis, transfer, and devices of single- and few-layer graphene by chemical vapor deposition *IEEE Trans. Nanotechnol.* **8** 135–8
[24] Li X *et al* 2009 Large-area synthesis of high-quality and uniform graphene films on copper foils *Science* **324** 1312–4
[25] Kim K S, Zhao Y, Jang H, Lee S Y, Kim J M, Kim K S, Ahn J-H, Kim P, Choi J-Y and Hong B H 2009 Large-scale pattern growth of graphene films for stretchable transparent electrodes *Nature* **457** 706–10
[26] Reina A, Jia X, Ho J, Nezich D, Son H, Bulovic V, Dresselhaus M S and Kong J 2009 Large area, few-layer graphene films on arbitrary substrates by chemical vapor deposition *Nano Lett.* **9** 30–35
[27] Okamoto H, Schlesinger M E and Mueller E M 2016 *ASM Handbook W Volume 3 Alloy Phase Diagrams* (Materials Park, OH: ASM International) (https://doi.org/10.31399/asm.hb.v03.9781627081634)
[28] Losurdo M, Giangregorio M M, Capezzuto P and Bruno G 2011 Graphene CVD growth on copper and nickel: role of hydrogen in kinetics and structure *Phys. Chem. Chem. Phys.* **13** 20836–43
[29] Sutter P W, Flege J-I and Sutter E A 2008 Epitaxial graphene on ruthenium *Nat. Mater.* **7** 406–11
[30] Coraux J, N'Diaye A T, Busse C and Michely T 2008 Structural coherency of graphene on Ir(111) *Nano Lett.* **8** 565–70
[31] Sutter P, Sadowski J T and Sutter E 2009 Graphene on Pt(111): growth and substrate interaction *Phys. Rev.* B **80** 245411
[32] An H, Lee W-J and Jung J 2011 Graphene synthesis on Fe foil using thermal CVD *Curr. Appl. Phys.* **11** S81–S85
[33] Varykhalov A and Rader O 2009 Graphene grown on Co(0001) films and islands: electronic structure and its precise magnetization dependence *Phys. Rev.* B **80** 035437
[34] Wang S M, Pei Y H, Wang X, Wang H, Meng Q N, Tian H W, Zheng X L, Zheng W T and Liu Y C 2010 Synthesis of graphene on a polycrystalline Co film by radio-frequency plasma-enhanced chemical vapour deposition *J. Phys. D: Appl. Phys.* **43** 455402
[35] Kwon S-Y, Ciobanu C V, Petrova V, Shenoy V B, Bareño J, Gambin V, Petrov I and Kodambaka S 2009 Growth of semiconducting graphene on palladium *Nano Lett.* **9** 3985–90
[36] Miniussi E *et al* 2011 Thermal stability of corrugated epitaxial graphene grown on Re(0001) *Phys. Rev. Lett.* **106** 216101
[37] Fan X, Wagner S, Schädlich P, Speck F, Kataria S, Haraldsson T, Seyller T, Lemme M C and Niklaus F 2018 Direct observation of grain boundaries in graphene through vapor hydrofluoric acid (VHF) exposure *Sci. Adv.* **4** 1–10
[38] Chen S, Ji H, Chou H, Li Q, Li H, Suk J W, Piner R, Liao L, Cai W and Ruoff R S 2013 Millimeter-size single-crystal graphene by suppressing evaporative loss of Cu during low pressure chemical vapor deposition *Adv. Mater.* **25** 2062–5

[39] Yan Z, Lin J, Peng Z, Sun Z, Zhu Y, Li L, Xiang C, Samuel E L, Kittrell C and Tour J M 2012 Toward the synthesis of wafer-scale single-crystal graphene on copper foils *ACS Nano* **6** 9110–7
[40] Hao Y *et al* 2013 The role of surface oxygen in the growth of large single-crystal graphene on copper *Science* **342** 720–3
[41] Ibrahim A, Nadhreen G, Akhtar S, Kafiah F M and Laoui T 2017 Study of the impact of chemical etching on Cu surface morphology, graphene growth and transfer on SiO2/Si substrate *Carbon* **123** 402–14
[42] Yu H K, Balasubramanian K, Kim K, Lee J-L, Maiti M, Ropers C, Krieg J, Kern K and Wodtke A M 2014 Chemical vapor deposition of graphene on a "peeled-off" epitaxial Cu(111) foil: a simple approach to improved properties *ACS Nano* **8** 8636–43
[43] Han G H, Güneş F, Bae J J, Kim E S, Chae S J, Shin H-J, Choi J-Y, Pribat D and Lee Y H 2011 Influence of copper morphology in forming nucleation seeds for graphene growth *Nano Lett.* **11** 4144–8
[44] Lin L, Sun L, Zhang J, Sun J, Koh A L, Peng H and Liu Z 2016 Rapid growth of large single-crystalline graphene via second passivation and multistage carbon supply *Adv. Mater.* **28** 4671–7
[45] Nguyen V L *et al* 2015 Seamless stitching of graphene domains on polished copper (111) foil *Adv. Mater.* **27** 1376–82
[46] Pan Y, Liu Y, Lu X, Pan G and Luo J 2012 The role of hydroxyethyl cellulose (HEC) in the chemical mechanical planarization of copper *J. Electrochem. Soc.* **159** H329–H334
[47] Mohsin A *et al* 2013 Synthesis of millimeter-size hexagon-shaped graphene single crystals on resolidified copper *ACS Nano* **7** 8924–31
[48] Li X, Magnuson C W, Venugopal A, Tromp R M, Hannon J B, Vogel E M, Colombo L and Ruoff R S 2011 Large-area graphene single crystals grown by low-pressure chemical vapor deposition of methane on copper *J. Am. Chem. Soc.* **133** 2816–9
[49] Strudwick A J, Weber N E, Schwab M G, Kettner M, Weitz R T, Wünsch J R, Müllen K and Sachdev H 2015 Chemical vapor deposition of high quality graphene films from carbon dioxide atmospheres *ACS Nano* **9** 31–42
[50] Gao L *et al* 2012 Repeated growth and bubbling transfer of graphene with millimetre-size single-crystal grains using platinum *Nat. Commun.* **3** 699
[51] Zhou H, Yu W J, Liu L, Cheng R, Chen Y, Huang X, Liu Y, Wang Y, Huang Y and Duan X 2013 Chemical vapour deposition growth of large single crystals of monolayer and bilayer graphene *Nat. Commun.* **4** 2096
[52] Wang H *et al* 2016 Surface monocrystallization of copper foil for fast growth of large single-crystal graphene under free molecular flow *Adv. Mater.* **28** 8968–74
[53] Geng D, Wu B, Guo Y, Huang L, Xue Y, Chen J, Yu G, Jiang L, Hu W and Liu Y 2012 Uniform hexagonal graphene flakes and films grown on liquid copper surface *Proc. Natl Acad. Sci. USA* **109** 7992–6
[54] Bae S *et al* 2010 Roll-to-roll production of 30-inch graphene films for transparent electrodes *Nat. Nanotechnol.* **5** 574–8
[55] Nguyen V L *et al* 2016 Wafer-scale single-crystalline AB-stacked bilayer graphene *Adv. Mater.* **28** 8177–83
[56] Wang B, Caffio M, Bromley C, Früchtl H and Schaub R 2010 Coupling epitaxy, chemical bonding, and work function at the local scale in transition metal-supported graphene *ACS Nano* **4** 5773–82
[57] Gao L, Guest J R and Guisinger N P 2010 Epitaxial graphene on Cu(111) *Nano Lett.* **10** 3512–6
[58] Iwasaki T, Park H J, Konuma M, Lee D S, Smet J H and Starke U 2011 Long-range ordered single-crystal graphene on high-quality heteroepitaxial Ni thin films grown on MgO(111) *Nano Lett.* **11** 79–84
[59] Gao M, Pan Y, Huang L, Hu H, Zhang L Z, Guo H M, Du S X and Gao H-J 2011 Epitaxial growth and structural property of graphene on Pt(111) *Appl. Phys. Lett.* **98** 033101
[60] Wofford J M, Starodub E, Walter A L, Nie S, Bostwick A, Bartelt N C, Thürmer K, Rotenberg E, McCarty K F and Dubon O D 2012 Extraordinary epitaxial alignment of graphene islands on Au(111) *New J. Phys.* **14** 053008
[61] N'Diaye A T *et al* 2009 *In situ* observation of stress relaxation in epitaxial graphene *New J. Phys.* **11** 113056
[62] Gotterbarm K, Zhao W, Höfert O, Gleichweit C, Papp C and Steinrück H-P 2013 Growth and oxidation of graphene on Rh(111) *Phys. Chem. Chem. Phys.* **15** 19625
[63] Lee J-H *et al* 2014 Wafer-scale growth of single-crystal monolayer graphene on reusable hydrogen-terminated germanium *Science* **344** 286–9
[64] Wu Y *et al* 2012 Synthesis of large-area graphene on molybdenum foils by chemical vapor deposition *Carbon* **50** 5226–31
[65] Wu T *et al* 2016 Fast growth of inch-sized single-crystalline graphene from a controlled single nucleus on Cu–Ni alloys *Nat. Mater.* **15** 43–7
[66] Li P, Wei W, Zhang M, Mei Y, Chu P K, Xie X, Yuan Q and Di Z 2020 Wafer-scale growth of single-crystal graphene on vicinal Ge(001) substrate *Nano Today* **34** 100908
[67] Wang T, Li P, Hu X, Gao M, Di Z, Xue Z and Zhang M 2020 Wafer-scale fabrication of single-crystal graphene on Ge(1 1 0) substrate by optimized CH_4/H_2 ratio *Appl. Surf. Sci.* **529** 147066
[68] Burton O J, Massabuau F C-P, Veigang-Radulescu V-P, Brennan B, Pollard A J and Hofmann S 2020 Integrated wafer scale growth of single crystal metal films and high quality graphene *ACS Nano* **14** 13593–601
[69] Suk J W, Kitt A, Magnuson C W, Hao Y, Ahmed S, An J, Swan A K, Goldberg B B and Ruoff R S 2011 Transfer of CVD-grown monolayer graphene onto arbitrary substrates *ACS Nano* **5** 6916–24
[70] Lock E H *et al* 2012 High-quality uniform dry transfer of graphene to polymers *Nano Lett.* **12** 102–7
[71] Chen Y, Gong X and Gai J 2016 Progress and challenges in transfer of large-area graphene films *Adv. Sci.* **3** 1500343
[72] De Fazio D *et al* 2019 High-mobility, wet-transferred graphene grown by chemical vapor deposition *ACS Nano* **13** 8926–35
[73] Ismach A, Druzgalski C, Penwell S, Schwartzberg A, Zheng M, Javey A, Bokor J and Zhang Y 2010 Direct chemical vapor deposition of graphene on dielectric surfaces *Nano Lett.* **10** 1542–8
[74] Rümmeli M H, Bachmatiuk A, Scott A, Börrnert F, Warner J H, Hoffman V, Lin J-H, Cuniberti G and Büchner B 2010 Direct low-temperature nanographene CVD synthesis over a dielectric insulator *ACS Nano* **4** 4206–10
[75] Gumi K, Ohno Y, Maehashi K, Inoue K and Matsumoto K 2012 Direct synthesis of graphene on SiO_2 substrates by transfer-free processes *Japan. J. Appl. Phys.* **51** 06FD12
[76] Kim Y J *et al* 2012 Low-temperature growth and direct transfer of graphene-graphitic carbon films on flexible plastic substrates *Nanotechnology* **23** 344016
[77] Kaplas T, Sharma D and Svirko Y 2012 Few-layer graphene synthesis on a dielectric substrate *Carbon* **50** 1503–9
[78] Li Y, Zhao Y, Chen Y, Chen Y, Zhou D and Zhao Z 2020 Direct synthesis of single-layer graphene films on quartz substrate by a nanoparticle-assisted method *Appl. Surf. Sci.* **529** 147082
[79] Chen C Y, Dai D, Chen G X, Yu J H, Nishimura K, Lin C T, Jiang N and Zhan Z L 2015 Rapid growth of single-layer graphene on the insulating substrates by thermal CVD *Appl. Surf. Sci.* **346** 41–5
[80] Xu S C, Man B Y, Jiang S Z, Chen C S, Yang C, Liu M, Gao X G, Sun Z C and Zhang C 2013 Direct synthesis of graphene on SiO_2 substrates by chemical vapor deposition *CrystEngComm* **15** 1840–4

[81] Su C Y et al 2011 Direct formation of wafer scale graphene thin layers on insulating substrates by chemical vapor deposition *Nano Lett.* **11** 3612–6
[82] Zheng S, Zhong G, Wu X, D'Arsiè L and Robertson J 2017 Metal-catalyst-free growth of graphene on insulating substrates by ammonia-assisted microwave plasma-enhanced chemical vapor deposition *RSC Adv.* **7** 33185–93
[83] Murakami K, Tanaka S, Hirukawa A, Hiyama T, Kuwajima T, Kano E, Takeguchi M and Fujita J I 2015 Direct synthesis of large area graphene on insulating substrate by gallium vapor-assisted chemical vapor deposition *Appl. Phys. Lett.* **106** 093112
[84] Vishwakarma R, Zhu R, Abuelwafa A A, Mabuchi Y, Adhikari S, Ichimura S, Soga T and Umeno M 2019 Direct synthesis of large-area graphene on insulating substrates at low temperature using microwave plasma CVD *ACS Omega* **4** 11263–70
[85] Muñoz R, Munuera C, Martínez J I, Azpeitia J, Gómez-Aleixandre C and García-Hernández M 2017 Low temperature metal free growth of graphene on insulating substrates by plasma assisted chemical vapor deposition *2D Mater.* **4** 015009
[86] Yan Z, Peng Z, Sun Z, Yao J, Zhu Y, Liu Z, Ajayan P M and Tour J M 2011 Growth of bilayer graphene on insulating substrates *ACS Nano* **5** 8187–92
[87] Ding X, Ding G, Xie X, Huang F and Jiang M 2011 Direct growth of few layer graphene on hexagonal boron nitride by chemical vapor deposition *Carbon* **49** 2522–5
[88] Dong Y, Guo S, Mao H, Xu C, Xie Y, Deng J, Wang L, Du Z, Xiong F and Sun J 2020 *In situ* growth of CVD graphene directly on dielectric surface toward application *ACS Appl. Electron. Mater.* **2** 238–46
[89] Sun J et al 2014 Direct growth of high-quality graphene on high-k dielectric $SrTiO_3$ substrates *J. Am. Chem. Soc.* **136** 6574–7
[90] Song H J, Son M, Park C, Lim H, Levendorf M P, Tsen A W, Park J and Choi H C 2012 Large scale metal-free synthesis of graphene on sapphire and transfer-free device fabrication *Nanoscale* **4** 3050–4
[91] Wu Z et al 2016 A fast transfer-free synthesis of high-quality monolayer graphene on insulating substrates by a simple rapid thermal treatment *Nanoscale* **8** 2594–600
[92] Wang D, Tian H, Yang Y, Xie D, Ren T L and Zhang Y 2013 Scalable and direct growth of graphene micro ribbons on dielectric substrates *Sci. Rep.* **3** 1–7
[93] Wang H, Xue X, Jiang Q, Wang Y, Geng D, Cai L, Wang L, Xu Z and Yu G 2019 Primary nucleation-dominated chemical vapor deposition growth for uniform graphene monolayers on dielectric substrate *J. Am. Chem. Soc.* **141** 11004–8
[94] Shin J H, Kim S H, Kwon S S and Il Park W 2018 Direct CVD growth of graphene on three-dimensionally-shaped dielectric substrates *Carbon* **129** 785–9
[95] Serrano I G, Panda J, Edvinsson T and Kamalakar M V 2020 Flexible transparent graphene laminates: via direct lamination of graphene onto polyethylene naphthalate substrates *Nanoscale Adv.* **2** 3156–63
[96] Han M Y, Özyilmaz B, Zhang Y and Kim P 2007 Energy band-gap engineering of graphene nanoribbons *Phys. Rev. Lett.* **98** 206805
[97] Dayen J-F, Mahmood A, Golubev D S, Roch-Jeune I, Salles P and Dujardin E 2008 Side-gated transport in focused-ion-beam-fabricated multilayered graphene nanoribbons *Small* **4** 716–20
[98] Chen Z, Narita A and Müllen K 2020 Graphene nanoribbons: on-surface synthesis and integration into electronic devices *Adv. Mater.* **32** 2001893
[99] Stampfer C, Güttinger J, Hellmüller S, Molitor F, Ensslin K and Ihn T 2009 Energy gaps in etched graphene nanoribbons *Phys. Rev. Lett.* **102** 056403
[100] Lemme M C 2014 Graphene and 2D layer devices for more moore and more-than-moore applications *Beyond-CMOS Nanodevices* vol 2 (Hoboken, NJ, USA: John Wiley & Sons, Inc.) pp 97–116
[101] Huyghebaert C et al 2019 2D materials: roadmap to CMOS integration *Tech. Dig.—Int. Electron Devices Meet. IEDM* (Institute of Electrical and Electronics Engineers Inc.) pp 22.1.1–4
[102] Pospischil A, Humer M, Furchi M M, Bachmann D, Guider R, Fromherz T and Mueller T 2013 CMOS-compatible graphene photodetector covering all optical communication bands *Nat. Photonics* **7** 892–6
[103] Pandey H et al 2018 All CVD boron nitride encapsulated graphene FETs with CMOS compatible metal edge contacts *IEEE Trans. Electron Devices* **65** 4129–34
[104] Gan X, Shiue R J, Gao Y, Meric I, Heinz T F, Shepard K, Hone J, Assefa S and Englund D 2013 Chip-integrated ultrafast graphene photodetector with high responsivity *Nat. Photonics* **7** 883–7
[105] Neumaier D, Pindl S and Lemme M C 2019 Integrating graphene into semiconductor fabrication lines *Nat. Mater.* **18** 525–9
[106] Jariwala D, Marks T J and Hersam M C 2017 Mixed-dimensional van der Waals heterostructures *Nat. Mater.* **16** 170–81
[107] Liu Y, Weiss N O, Duan X, Cheng H-C, Huang Y and Duan X 2016 Van der Waals heterostructures and devices *Nat. Rev. Mater.* **1** 16042
[108] Anichini C, Czepa W, Pakulski D, Aliprandi A, Ciesielski A and Samorì P 2018 Chemical sensing with 2D materials *Chem. Soc. Rev.* **47** 4860–908
[109] Gobbi M et al 2017 Periodic potentials in hybrid van der Waals heterostructures formed by supramolecular lattices on graphene *Nat. Commun.* **8** 14767
[110] Schedin F, Geim A K, Morozov S V, Hill E W, Blake P, Katsnelson M I and Novoselov K S 2007 Detection of individual gas molecules adsorbed on graphene *Nat. Mater.* **6** 652–5
[111] Lee W H, Park J, Sim S H, Lim S, Kim K S, Hong B H and Cho K 2011 Surface-directed molecular assembly of pentacene on monolayer graphene for high-performance organic transistors *J. Am. Chem. Soc.* **133** 4447–54
[112] Mahmood A et al 2019 Tuning graphene transistors through: ad hoc electrostatics induced by a nanometer-thick molecular underlayer *Nanoscale* **11** 19705–12
[113] Seo S, Min M, Lee S M and Lee H 2013 Photo-switchable molecular monolayer anchored between highly transparent and flexible graphene electrodes *Nat. Commun.* **4** 1–7
[114] Dugay J, Aarts M, Giménez-Marqués M, Kozlova T, Zandbergen H W, Coronado E and Van Der Zant H S J 2017 Phase transitions in spin-crossover thin films probed by graphene transport measurements *Nano Lett.* **17** 186–93
[115] Konstantinov N et al 2021 Electrical readout of light-induced spin transition in thin film spin crossover/graphene heterostructure *J. Mater. Chem. C* **9** 2712–20
[116] Zheng Y, Ni G X, Toh C T, Zeng M G, Chen S T, Yao K and Özyilmaz B 2009 Gate-controlled nonvolatile graphene-ferroelectric memory *Appl. Phys. Lett.* **94** 163505
[117] Zhu Z, Zhang B, Chen X, Qian X and Qi J 2020 Electric field control of molecular magnetic state by two-dimensional ferroelectric heterostructure engineering *Appl. Phys. Lett.* **117** 082902
[118] Wang Z, Tang C, Sachs R, Barlas Y and Shi J 2015 Proximity-induced ferromagnetism in graphene revealed by the anomalous Hall effect *Phys. Rev. Lett.* **114** 016603

[119] Song G, Ranjbar M, Daughton D R and Kiehl R A 2019 Nanoparticle-induced anomalous Hall effect in graphene *Nano Lett.* **19** 7112–8
[120] Britnell L *et al* 2012 Field-effect tunneling transistor based on vertical graphene heterostructures *Science* **335** 947–50
[121] Liu Y, Zhou H, Cheng R, Yu W, Huang Y and Duan X 2014 Highly flexible electronics from scalable vertical thin film transistors *Nano Lett.* **14** 1413–8
[122] Mouafo L D N *et al* 2021 0D/2D heterostructures vertical single electron transistor *Adv. Funct. Mater.* **31** 2008255
[123] Mouafo L D N *et al* 2018 Anisotropic magneto-coulomb properties of 2D-0D heterostructure single electron device *Adv. Mater.* **30** 1802478
[124] Florian Godel L D N M 2017 Conductance oscillations in a graphene/nanocluster hybrid material: toward large-area single-electron devices *Adv. Mater.* **29** 1604837
[125] Yang H, Heo J, Park S, Song H J, Seo D H, Byun K-E, Kim P, Yoo I, Chung H-J and Kim K 2012 Graphene barristor, a triode device with a gate-controlled schottky barrier *Science* **336** 1140–3
[126] Vaziri S, Lupina G, Henkel C, Smith A D, Ostling M, Dabrowski J, Lippert G, Mehr W and Lemme M C 2013 A graphene-based hot electron transistor *Nano Lett.* **13** 1435–9
[127] Konstantatos G, Badioli M, Gaudreau L, Osmond J, Bernechea M, De Arquer F P G, Gatti F and Koppens F H L 2012 Hybrid graphene–quantum dot phototransistors with ultrahigh gain *Nat. Nanotechnol.* **7** 363–8
[128] Noumbé U N *et al* 2020 Reconfigurable 2D/0D p–n graphene/HgTe nanocrystal heterostructure for infrared detection *ACS Nano* **14** 4567–76
[129] Grotevent M J, Hail C U, Yakunin S, Bachmann D, Calame M, Poulikakos D, Kovalenko M V and Shorubalko I 2021 Colloidal HgTe quantum dot/graphene phototransistor with a spectral sensitivity beyond 3 μm *Adv. Sci.* **8** 2003360
[130] Guan X *et al* 2021 Recent progress in short- to long-wave infrared photodetection using 2D materials and heterostructures *Adv. Opt. Mater.* **9** 2001708
[131] Nikitskiy I, Goossens S, Kufer D, Lasanta T, Navickaite G, Koppens F H L and Konstantatos G 2016 Integrating an electrically active colloidal quantum dot photodiode with a graphene phototransistor *Nat. Commun.* **7** 11954
[132] Gréboval C *et al* 2020 Gate tunable vertical geometry phototransistor based on infrared HgTe nanocrystals *Appl. Phys. Lett.* **117** 251104
[133] Ferrari A C *et al* 2015 Science and technology roadmap for graphene, related two-dimensional crystals, and hybrid systems *Nanoscale* **7** 4598–810
[134] Ruhl G, Wittmann S, Koenig M and Neumaier D 2017 The integration of graphene into microelectronic devices *Beilstein J. Nanotechnol.* **8** 1056–64
[135] Morozov S V, Novoselov K S, Katsnelson M I, Schedin F, Elias D C, Jaszczak J A and Geim A K 2008 Giant intrinsic carrier mobilities in graphene and its bilayer *Phys. Rev. Lett.* **100** 016602
[136] Castro E V, Ochoa H, Katsnelson M I, Gorbachev R V, Elias D C, Novoselov K S, Geim A K and Guinea F 2010 Limits on charge carrier mobility in suspended graphene due to flexural phonons *Phys. Rev. Lett.* **105** 266601
[137] Bolotin K I, Sikes K J, Hone J, Stormer H L and Kim P 2008 Temperature-dependent transport in suspended graphene *Phys. Rev. Lett.* **101** 096802
[138] Du X, Skachko I, Barker A and Andrei E Y 2008 Approaching ballistic transport in suspended graphene *Nat. Nanotechnol.* **3** 491–5
[139] Brown M A, Crosser M S, Leyden M R, Qi Y and Minot E D 2016 Measurement of high carrier mobility in graphene in an aqueous electrolyte environment *Appl. Phys. Lett.* **109** 093104
[140] Gannett W, Regan W, Watanabe K, Taniguchi T, Crommie M F and Zettl A 2011 Boron nitride substrates for high mobility chemical vapor deposited graphene *Appl. Phys. Lett.* **98** 242105
[141] Pezzini S, Mišeikis V, Pace S, Rossella F, Watanabe K, Taniguchi T and Coletti C 2020 High-quality electrical transport using scalable CVD graphene *2D Mater.* **7** 041003
[142] Ni G X *et al* 2012 Quasi-periodic nanoripples in graphene grown by chemical vapor deposition and its impact on charge transport *ACS Nano* **6** 1158–64
[143] Van Veldhoven Z A, Alexander-Webber J A, Sagade A A, Braeuninger-Weimer P and Hofmann S 2016 Electronic properties of CVD graphene: the role of grain boundaries, atmospheric doping, and encapsulation by ALD *Phys. Status Solidi* **253** 2321–5
[144] Tőke C, Lammert P E, Crespi V H and Jain J K 2006 Fractional quantum Hall effect in graphene *Phys. Rev.* B **74** 235417
[145] Du X, Skachko I, Duerr F, Luican A and Andrei E Y 2009 Fractional quantum Hall effect and insulating phase of Dirac electrons in graphene *Nature* **462** 192–5
[146] Matsoso B, Hao W, Li Y, Vuillet-a-ciles V, Garnier V, Steyer P, Toury B, Marichy C and Journet C 2020 Synthesis of hexagonal boron nitride 2D layers using polymer derived ceramics route and derivatives *J. Phys. Mater.* **3** 034002
[147] Rigosi A F, Levy A L, Snure M R and Glavin N R 2021 Turn of the decade: versatility of 2D hexagonal boron nitride *J. Phys. Mater.* **4** 032003
[148] Kim B J, Jang H, Lee S K, Hong B H, Ahn J H and Cho J H 2010 High-performance flexible graphene field effect transistors with ion gel gate dielectrics *Nano Lett.* **10** 3464–6
[149] Lu C C, Lin Y C, Yeh C H, Huang J C and Chiu P W 2012 High mobility flexible graphene field-effect transistors with self-healing gate dielectrics *ACS Nano* **6** 4469–74
[150] Lee J, Ha T J, Li H, Parrish K N, Holt M, Dodabalapur A, Ruoff R S and Akinwande D 2013 25 GHz embedded-gate graphene transistors with high-K dielectrics on extremely flexible plastic sheets *ACS Nano* **7** 7744–50
[151] Liang Y, Liang X, Zhang Z, Li W, Huo X and Peng L 2015 High mobility flexible graphene field-effect transistors and ambipolar radio-frequency circuits *Nanoscale* **7** 10954–62
[152] Yang X, Vorobiev A, Generalov A, Andersson M A and Stake J 2017 A flexible graphene terahertz detector *Appl. Phys. Lett.* **111** 021102
[153] Wang Z, Shaygan M, Otto M, Schall D and Neumaier D 2016 Flexible Hall sensors based on graphene *Nanoscale* **8** 7683–7
[154] Uzlu B, Wang Z, Lukas S, Otto M, Lemme M C and Neumaier D 2019 Gate-tunable graphene-based Hall sensors on flexible substrates with increased sensitivity *Sci. Rep.* **9** 18059
[155] Fert A 2008 , Nobel Lecture: origin, development, and future of spintronics *Rev. Mod. Phys.* **80** 1517–30
[156] Parkin S S P, Hayashi M and Thomas L 2008 Magnetic domain-wall racetrack memory *Science* **320** 190–4
[157] Idzuchi H, Fukuma Y and Otani Y 2015 Spin transport in non-magnetic nano-structures induced by non-local spin injection *Physica* E **68** 239–63
[158] Hill E W, Geim A K, Novoselov K, Schedin F and Blake P 2006 Graphene spin valve devices *IEEE Trans. Magn.* **42** 2694–6
[159] Cho S, Chen Y-F and Fuhrer M S 2007 Gate-tunable graphene spin valve *Appl. Phys. Lett.* **91** 123105

[160] Ohishi M, Shiraishi M, Nouchi R, Nozaki T, Shinjo T and Suzuki Y 2007 Spin injection into a graphene thin film at room temperature *Japan. J. Appl. Phys.* **46** L605–7
[161] Johnson M and Silsbee R H 1985 Interfacial charge-spin coupling: injection and detection of spin magnetization in metals *Phys. Rev. Lett.* **55** 1790–3
[162] Han W, Pi K, McCreary K M, Li Y, Wong J J I, Swartz A G and Kawakami R K 2010 Tunneling spin injection into single layer graphene *Phys. Rev. Lett.* **105** 167202
[163] Kamalakar M V, Dankert A, Bergsten J, Ive T and Dash S P 2014 Enhanced tunnel spin injection into graphene using chemical vapor deposited hexagonal boron nitride *Sci. Rep.* **4** 6146
[164] Kamalakar M V, Dankert A, Bergsten J, Ive T and Dash S P 2014 Spintronics with graphene-hexagonal boron nitride van der Waals heterostructures *Appl. Phys. Lett.* **105** 212405
[165] Guimarães M H D, Zomer P J, Ingla-Aynés J, Brant J C, Tombros N and Van Wees B J 2014 Controlling spin relaxation in hexagonal BN-encapsulated graphene with a transverse electric field *Phys. Rev. Lett.* **113** 086602
[166] Ingla-Aynés J, Guimarães M H D, Meijerink R J, Zomer P J and Van Wees B J 2015 24 μ m spin relaxation length in boron nitride encapsulated bilayer graphene *Phys. Rev.* B **92** 201410
[167] Volmer F, Drögeler M, Maynicke E, Von Den Driesch N, Boschen M L, Güntherodt G and Beschoten B 2013 Role of MgO barriers for spin and charge transport in Co/MgO/graphene nonlocal spin-valve devices *Phys. Rev.* B **88** 161405
[168] Avsar A *et al* 2011 Towards wafer scale fabrication of graphene based spin valve devices *Nano Lett.* **11** 2363–8
[169] Ochoa H, Castro Neto A H and Guinea F 2012 Elliot-Yafet mechanism in graphene *Phys. Rev. Lett.* **108** 206808
[170] Zhang P and Wu M W 2012 Electron spin relaxation in graphene with random Rashba field: comparison of the D'yakonov–Perel' and Elliott–Yafet-like mechanisms *New J. Phys.* **14** 033015
[171] Huertas-Hernando D, Guinea F and Brataas A 2009 Spin-orbit-mediated spin relaxation in graphene *Phys. Rev. Lett.* **103** 146801
[172] Han W and Kawakami R K 2011 Spin relaxation in single-layer and bilayer graphene *Phys. Rev. Lett.* **107** 047207
[173] Zomer P J, Guimarães M H D, Tombros N and Van Wees B J 2012 Long-distance spin transport in high-mobility graphene on hexagonal boron nitride *Phys. Rev.* B **86** 161416
[174] Stecklein G, Crowell P A, Li J, Anugrah Y, Su Q and Koester S J 2016 Contact-induced spin relaxation in graphene nonlocal spin valves *Phys. Rev. Appl.* **6** 054015
[175] Kamalakar M V, Groenveld C, Dankert A and Dash S P 2015 Long distance spin communication in chemical vapour deposited graphene *Nat. Commun.* **6** 6766
[176] Van Tuan D, Ortmann F, Soriano D, Valenzuela S O and Roche S 2014 Pseudospin-driven spin relaxation mechanism in graphene *Nat. Phys.* **10** 857–63
[177] Cummings A W and Roche S 2016 Effects of dephasing on spin lifetime in ballistic spin-orbit materials *Phys. Rev. Lett.* **116** 086602
[178] Kochan D, Gmitra M and Fabian J 2014 Spin relaxation mechanism in graphene: resonant scattering by magnetic impurities *Phys. Rev. Lett.* **112** 116602
[179] Lundeberg M, Yang R, Renard J and Folk J 2013 Defect-mediated spin relaxation and dephasing in graphene *Phys. Rev. Lett.* **110** 156601
[180] Panda J, Ramu M, Karis O, Sarkar T and Kamalakar M V 2020 Ultimate spin currents in commercial chemical vapor deposited graphene *ACS Nano* **14** 12771–80
[181] Huang P Y *et al* 2011 Grains and grain boundaries in single-layer graphene atomic patchwork quilts *Nature* **469** 389–92
[182] Kim K, Lee Z, Regan W, Kisielowski C, Crommie M F and Zettl A 2011 Grain boundary mapping in polycrystalline graphene *ACS Nano* **5** 2142–6
[183] Huertas-Hernando D, Guinea F and Brataas A 2007 Spin relaxation times in disordered graphene *Eur. Phys. J. Spec. Top.* **148** 177–81
[184] Fratini S, Gosálbez-Martínez D, Merodio Cámara P and Fernández-Rossier J 2013 Anisotropic intrinsic spin relaxation in graphene due to flexural distortions *Phys. Rev.* B **88** 115426
[185] Gebeyehu Z M, Parui S, Sierra J F, Timmermans M, Esplandiu M J, Brems S, Huyghebaert C, Garello K, Costache M V and Valenzuela S O 2019 Spin communication over 30 μm long channels of chemical vapor deposited graphene on SiO 2 *2D Mater.* **6** 034003
[186] Cummings A W, Dubois S-M-M, Charlier J-C and Roche S 2019 Universal spin diffusion length in polycrystalline graphene *Nano Lett.* **19** 7418–26
[187] Jeong J-S, Shin J and Lee H-W 2011 Curvature-induced spin-orbit coupling and spin relaxation in a chemically clean single-layer graphene *Phys. Rev.* B **84** 195457
[188] Dugaev V K, Sherman E Y and Barnaś J 2011 Spin dephasing and pumping in graphene due to random spin-orbit interaction *Phys. Rev.* B **83** 085306
[189] Whelan P R *et al* 2020 Fermi velocity renormalization in graphene probed by terahertz time-domain spectroscopy *2D Mater.* **7** 035009
[190] Serrano I G, Panda J, Denoel F, Vallin Ö, Phuyal D, Karis O and Kamalakar M V 2019 Two-dimensional flexible high diffusive spin circuits *Nano Lett.* **19** 666–73
[191] Muscas G, Jönsson P E, Serrano I G, Vallin Ö and Kamalakar M V 2021 Ultralow magnetostrictive flexible ferromagnetic nanowires *Nanoscale* **13** 6043–52
[192] Calado V E, Zhu S-E, Goswami S, Xu Q, Watanabe K, Taniguchi T, Janssen G C A M and Vandersypen L M K 2014 Ballistic transport in graphene grown by chemical vapor deposition *Appl. Phys. Lett.* **104** 23103
[193] Schmitz M, Engels S, Banszerus L, Watanabe K, Taniguchi T, Stampfer C and Beschoten B 2017 High mobility dry-transferred CVD bilayer graphene *Appl. Phys. Lett.* **110** 263110
[194] Banszerus L, Schmitz M, Engels S, Dauber J, Oellers M, Haupt F, Watanabe K, Taniguchi T, Beschoten B and Stampfer C n.d. Ultrahigh-mobility graphene devices from chemical vapor deposition on reusable copper *Sci. Adv.* **1** e1500222
[195] Drögeler M, Franzen C, Volmer F, Pohlmann T, Banszerus L, Wolter M, Watanabe K, Taniguchi T, Stampfer C and Beschoten B 2016 Spin lifetimes exceeding 12 ns in graphene nonlocal spin valve devices *Nano Lett.* **16** 3533–9
[196] Dro M, Volmer F, Wolter M, Terre B, Watanabe K, Taniguchi T, Gu G, Stampfer C and Beschoten B 2014 Nanosecond spin lifetimes in single-and few-layer graphene−hbn heterostructures at room temperature *Nano Lett.* **14** 6050–5
[197] Khokhriakov D, Karpiak B, Hoque A M and Dash S P 2020 Two-dimensional spintronic circuit architectures on large scale graphene *Carbon* **161** 892–9
[198] Fu W, Makk P, Maurand R, Bräuninger M and Schönenberger C 2014 Large-scale fabrication of BN tunnel barriers for graphene spintronics *J. Appl. Phys.* **116** 074306

[199] Gurram M, Omar S, Zihlmann S, Makk P, Li Q C, Zhang Y F, Schönenberger C and Van Wees B J 2018 Spin transport in two-layer-CVD-hBN/graphene/hBN heterostructures *Phys. Rev.* B **97** 045411
[200] Drögeler M, Banszerus L, Volmer F, Taniguchi T, Watanabe K, Beschoten B and Stampfer C 2017 Dry-transferred CVD graphene for inverted spin valve devices *Appl. Phys. Lett.* **111** 152402
[201] Godel F, Kamalakar M V, Doudin B, Henry Y, Halley D and Dayen J-F 2014 Voltage-controlled inversion of tunnel magnetoresistance in epitaxial nickel/graphene/MgO/cobalt junctions *Appl. Phys. Lett.* **105** 152407
[202] Karpan V M, Giovannetti G, Khomyakov P, Talanana M, Starikov A A, Zwierzycki M, Van Den Brink J, Brocks G and Kelly P J 2007 Graphite and Graphene as Perfect Spin Filters *Phys. Rev. Lett.* **99** 176602
[203] Dayen J-F, Ray S J, Karis O, Vera-Marun I J and Kamalakar M V 2020 Two-dimensional van der Waals spinterfaces and magnetic-interfaces *Appl. Phys. Rev.* **7** 011303
[204] Dedkov Y S, Fonin M and Laubschat C 2008 A possible source of spin-polarized electrons: the inert graphene/Ni(111) system *Appl. Phys. Lett.* **92** 052506
[205] Dlubak B *et al* 2012 Graphene-passivated nickel as an oxidation-resistant electrode for spintronics *ACS Nano* **6** 10930–4
[206] Usachov D *et al* 2015 Observation of single-spin dirac fermions at the graphene/ferromagnet interface *Nano Lett.* **15** 2396–401
[207] Zhou G, Tang G, Li T, Pan G, Deng Z and Zhang F 2017 Graphene-passivated cobalt as a spin-polarized electrode: growth and application to organic spintronics *J. Phys. D: Appl. Phys.* **50** 095001
[208] Asshoff P U *et al* 2017 Magnetoresistance of vertical Co-graphene-NiFe junctions controlled by charge transfer and proximity-induced spin splitting in graphene *2D Mater.* **4** 031004
[209] Piquemal-Banci M *et al* 2020 Spin filtering by proximity effects at hybridized interfaces in spin-valves with 2D graphene barriers *Nat. Commun.* **11** 5670
[210] Kozhakhmetov A, Torsi R, Chen C Y and Robinson J A 2020 Scalable low-temperature synthesis of two-dimensional materials beyond graphene *J. Phys. Mater.* **4** 012001
[211] Mandyam S V, Kim H M and Drndić M 2020 Large area few-layer TMD film growths and their applications *J. Phys. Mater.* **3** 024008
[212] Giustino F *et al* 2021 The 2021 quantum materials roadmap *J. Phys. Mater.* **3** 042006
[213] Bora M and Deb P 2021 Magnetic proximity effect in two-dimensional van der Waals heterostructure *J. Phys. Mater.* **4** 034014
[214] Jiménez D, Cummings A W, Chaves F, Van Tuan D, Kotakoski J and Roche S 2014 Impact of graphene polycrystallinity on the performance of graphene field-effect transistors *Appl. Phys. Lett.* **104** 043509
[215] Mahmood A, Yang C-S, Dayen J-F, Park S, Kamalakar M V, Metten D, Berciaud S, Lee J-O and Doudin B 2015 Room temperature dry processing of patterned CVD graphene devices *Carbon* **86** 256–63